

Non-Markovian environment induced chaos in optomechanical system

You-Lin Xiang, Xinyu Zhao,* and Yan Xia†

Fujian Key Laboratory of Quantum Information and Quantum Optics (Fuzhou University), Fuzhou 350108, China and Department of Physics, Fuzhou University, Fuzhou 350108, China

In traditional research, chaos is frequently accompanied by non-linearity, which typically stems from non-linear interactions or external driving forces. However, in this paper, we present the chaotic behavior that is completely attributed to the non-linear back-reaction of non-Markovian environment. To be specific, we derive the dynamical equations of an optomechanical system and demonstrate that the non-linearity (cause of chaos) in the equations arises entirely from the time-domain convolutions (TDCs) induced by non-Markovian corrections. Under Markovian conditions, these TDCs are reduced into constants, thereby losing the nonlinearity and ultimately leading to the disappearance of chaos. Furthermore, we also observe chaos generation in the absence of optomechanical couplings, which further confirms that the non-Markovian effect is the sole inducement of chaos and the environmental parameters play important roles in the generation of chaos. We hope these results may open a new direction to investigate chaotic dynamics purely caused by non-Markovian environments.

I. INTRODUCTION

Chaos has been widely studied in many fields, such as neural networks [1], extreme event statistics [2, 3], and biophysics of chaotic self-organization [4]. The investigation of chaos not only advances our understanding of fundamental physics but also offers significant potential for a range of applications [5–34]. For example, chaos plays an important role in secret communications [5, 6], rapid generation of high-quality random bit sequences [8, 11], and chaos assisted computing [35].

Traditional theory believes that chaos arises from the nonlinear interactions within the system [36, 37]. Therefore, a significant amount of research focuses on the physical systems whose dynamics is governed by nonlinear equations. Optomechanical system is such an example that exhibits a wealth of nonlinear characteristics [38–52], originating from the interaction between the cavity mode and the mechanical oscillator. Therefore, optomechanical systems have become one of the candidate platforms for the study and exploration of classical and quantum chaos [53–58]. Over the past few years, extensive theoretical and experimental research has been conducted on optomechanical systems, for example, Hamiltonian chaos [53], loss-induced chaos [54], and intermittent chaos [57].

In the studies above and other traditional research [55–60] on chaos in optomechanical systems, the dynamical equations are always nonlinear. However, in this paper, we present chaotic behavior in an optomechanical system purely caused by the back-reaction of the non-Markovian environment. In our model, the dynamical equation is in a linear format, the non-linearity only arises from the time-domain convolutions (TDCs), satisfying a set of non-linear differential equations. It is proved that

those TDCs merely arises from the non-Markovian corrections to the coefficients in the master equation. Therefore, the chaotic behavior is an exclusive feature for non-Markovian case. In Markovian regime, the TDCs are reduced to constants resulting in the vanish of chaos.

To be specific, we investigate the dynamics of an optomechanical system with two movable mirrors beyond the Markov approximation. By employing the non-Markovian quantum state diffusion (NMQSD) approach [22, 61–68], the non-Markovian master equation is derived. Then, a set of dynamical equations are derived for physical observables. Although these dynamical equations are in linear form, the coefficients $F_i(t)$ (TDCs) in the dynamical equations satisfy another set of nonlinear differential equations when the non-Markovian correction is taken into consideration.

We employ the maximum Lyapunov exponent (LE) [36, 69, 70] to measure the chaotic behavior in the dynamical process and prove that chaos is only generated in non-Markovian regime. Analytical results confirm that both non-linearity and chaotic behavior arise purely from the TDCs in the dynamical equation, which implies non-Markovian correction is the only cause of chaos. In another word, the chaotic behavior is a unique feature in non-Markovian dynamics and never occurs in Markovian regime. All these results are also demonstrated in numerical simulations. Furthermore, we have also excluded the influence of optomechanical couplings on chaos generation. In the absence of optomechanical couplings, numerical results demonstrate that non-Markovian effect is the only cause of chaos.

From the perspective of physical pictures, in traditional research, non-linearity as a necessary condition for chaos comes from either the external driving force [71, 72] or intrinsic nonlinear interactions (reflected as nonlinear terms in the dynamical equations [37, 73]). In our research, the non-Markovian back-reaction from the environment becomes the provider of nonlinear effects. In summary, non-Markovian effects cause the non-linearity in TDCs, further introduce chaos in the dynamics of sys-

* xzhao@fzu.edu.cn

† xia-208@163.com

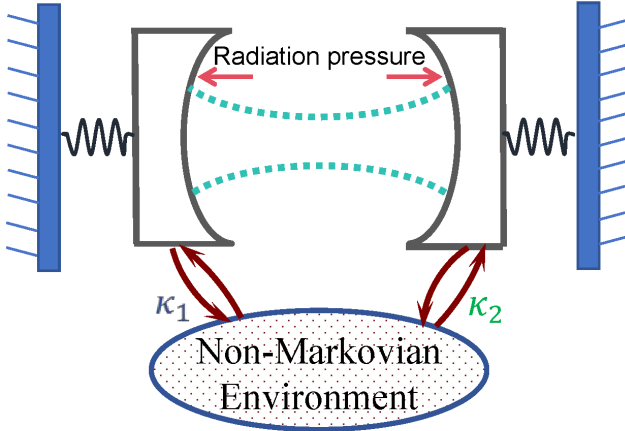


FIG. 1. Schematic diagram of double-mirror optomechanical system. An F-P cavity is coupled to two movable mirrors through the radiation pressure. Both mirrors are coupled to a non-Markovian common environment.

tem, even if the dynamical equation is in a linear format.

Last but not least, we have further studied the influence of several environmental parameters in the chaos generation process, such as the memory time, dissipation rate, and central frequency of the environment. Our research indicates that environmental factors can have a crucial impact on the generation of chaos. The non-Markovianity of the environment acts as a switch to control the generation and disappearance of chaos. We aspire that the findings presented in this paper could pave a novel way to delve into chaotic dynamics solely stemming from non-Markovian effects.

The paper is organized as follows. In Sec. II, we derive the non-Markovian master equation for the double-mirror optomechanical system. In Sec. III, we introduce the method of quantifying chaos and demonstrate that chaos can be only generated in non-Markovian regime. In Sec. IV, we show the influence of environmental parameters. Finally, conclusion and outlook are given in Sec. V.

II. NON-MARKOVIAN DYNAMICS OF DOUBLE-MIRROR OPTOMECHANICAL SYSTEM

A. Double-mirror optomechanical system with non-Markovian environment

As shown in Fig. 1, the system we considered is a double-mirror optomechanical system, which is an Fabry-Perot cavity with two reflective movable mirrors. The motions of two mirrors can be modeled as quantum harmonic oscillators, while the cavity field can be described by a light field. Therefore, the total Hamiltonian is written as (assuming $\hbar = 1$)

$$\hat{H}_{\text{tot}} = \hat{H}_{\text{S}} + \hat{H}_{\text{B}} + \hat{H}_{\text{int}}, \quad (1)$$

where

$$\hat{H}_{\text{S}} = \omega_c \hat{a}^\dagger \hat{a} + \sum_{j=1}^2 \omega_j (\hat{p}_j^2 + \hat{q}_j^2) + \sum_{j=1}^2 G_j \hat{a}^\dagger \hat{a} \hat{q}_j, \quad (2)$$

is the Hamiltonian for the double-mirror optomechanical system [74]. The position and momentum operators for the two mirrors are indicated by \hat{p}_j and \hat{q}_j ($j = 1, 2$), respectively, and the creation (annihilation) operators of the cavity mode are represented by \hat{a}^\dagger (\hat{a}). In Eq. (2), the term $G_j \hat{a}^\dagger \hat{a} \hat{q}_j$ represents the interaction between the radiation field and the two mirrors. Through radiation pressure, the positions of the two mirrors are coupled to the photon numbers in the cavity field with the coupling strength G_1 and G_2 , respectively.

A general bosonic common environment can be modeled as

$$\hat{H}_{\text{B}} = \sum_i \nu_i \hat{b}_i^\dagger \hat{b}_i, \quad (3)$$

where \hat{b}_i is the annihilation operator of the i^{th} mode. The interaction between system and environment can be described as

$$\hat{H}_{\text{int}} = \sum_i g_i (\kappa_1 \hat{q}_1 + \kappa_2 \hat{q}_2) (\hat{b}_i^\dagger + \hat{b}_i), \quad (4)$$

where $(\kappa_1 \hat{q}_1 + \kappa_2 \hat{q}_2)$ describes the collective interaction between system and environment with the dimensionless coefficients κ_1, κ_2 , respectively. The coupling strength to the i^{th} mode of the environment is g_i .

Here, we assume that the dissipation of the movable mirrors is the primary dissipative channel of the system and two mirrors are coupled to a common environment. This is the most common case because a massive object (mirror) loss its coherence much faster than light field. In practical cases, the leakage of the cavity is another source of dissipation. The corresponding discussion on cavity leakage is shown in Appendix C. Besides, the temperature of the environment also has a significant impact on the dynamics of the open system. The solution to the finite temperature case is presented in D.

The properties of the environment are mainly determined by the correlation function (see Appendix A 1 for details)

$$\alpha(t, s) = \sum_i |g_i|^2 e^{-i\nu_i(t-s)}. \quad (5)$$

Consider a continuous distribution of mode frequency, the summation over mode “ i ” can be replaced by the integration over frequency “ ν ” as

$$\alpha(t, s) = \int_0^\infty J(\nu) e^{-i\nu(t-s)} d\nu, \quad (6)$$

where $J(\nu) = |g(\nu)|^2$ is the spectrum density describing the coupling strength to the environmental modes with eigen-frequency ν . A commonly studied case is that

the coupling strengths for different modes are identical, namely $J(\nu) = \Gamma$, the correlation function becomes a delta-function $\alpha(t, s) = \frac{\Gamma}{2}\delta(t, s)$. This indicates the environment is memory-less, as it is often called “Markovian” environment.

In the most general case, the spectrum density $J(\nu)$ can be arbitrarily complicated. Here, we explore a widely studied case called the Lorentzian spectrum density [75–78]

$$J(\nu) = \frac{\Gamma\gamma^2/2\pi}{(\nu - \Omega)^2 + \gamma^2}, \quad (7)$$

where Ω is the central frequency of the environment. The coupling to the mode with $\nu = \Omega$ is the strongest, while the couplings are much weaker when the mode frequency ν is far away from Ω ($|\nu - \Omega| \gg \gamma$). Such a spectrum density $J(\nu)$ corresponds to the so-called Ornstein-Uhlenbeck (O-U) correlation function (assuming $\Gamma = 1$)

$$\alpha(t, s) = \int_0^\infty J(\nu)e^{-i\nu(t-s)}d\nu = \frac{\Gamma\gamma}{2}e^{-(\gamma+i\Omega)|t-s|}, \quad (8)$$

where the residue theorem is used in the calculation of the integral. Now, the physical meaning of the parameter γ is clear. Noticing that $1/\gamma$ has the unit of time, $\tau = 1/\gamma$ can somehow measure the memory time of the environment. When two points “ t ” and “ s ” in the time domain are separated much larger than the memory time $|t-s| \gg \tau$, their correlation is approaching zero, $\alpha(t, s) \rightarrow 0$. In O-U correlation function, the transition from Markovian to non-Markovian regime can be observed by tuning a single parameter γ . When $\gamma \rightarrow \infty$, the environment exhibits Markovian properties, while γ is small, the non-Markovian corrections become non-negligible.

Typically, other types of correlation functions can be decomposed into combinations of several O-U correlation functions, since an arbitrary function can be expanded into an exponential Fourier series. As an example given in Ref. [77], the widely used $1/f$ noise can be decomposed into many O-U noises. Here, we chose the O-U correlation function based on the need to show the transition from a Markovian to a non-Markovian regime by tuning a single parameter $\tau = 1/\gamma$.

B. Master equation and dynamical equations

By introducing normalized (Bargmann) coherent state [79, 80] $|z_i\rangle = e^{z_i\hat{b}_i^\dagger}|0\rangle$ as the basis to expand the

total state vector $|\psi_{\text{tot}}(t)\rangle$ (resides in the joint Hilbert space $\mathcal{H}_{\text{sys}} \otimes \mathcal{H}_{\text{env}}$), one can define a stochastic state vector belonging to the system’s Hilbert space \mathcal{H}_{sys} . Such a stochastic state vector is formally defined as $|\psi_t(z^*)\rangle \equiv \langle z|\psi_{\text{tot}}(t)\rangle$, where $|z\rangle \equiv \prod_i |z_i\rangle$ represents the collective coherent states of all the modes in environments (only residing in the environment’s Hilbert space \mathcal{H}_{env}). The inner product $\langle z|\psi_{\text{tot}}\rangle$ projects the total state onto the environmental modes, thereby stripping away environmental degrees of freedom and retaining only the system’s quantum state. According to the Schrödinger equation for the total system, the equation for the stochastic state vector $|\psi_t(z^*)\rangle$ can be derived as (see Appendix A 1 for details)

$$\begin{aligned} \frac{\partial}{\partial t}|\psi_t(z^*)\rangle &= [-i\hat{H}_{\text{S}} + (\kappa_1\hat{q}_1 + \kappa_2\hat{q}_2)z_t^* \\ &\quad - (\kappa_1^*\hat{q}_1 + \kappa_2^*\hat{q}_2)\int_0^t ds\alpha(t, s)\frac{\delta}{\delta z_s^*}]|\psi_t(z^*)\rangle, \end{aligned} \quad (9)$$

which is called the NMQSD equation [61, 63]. In Eq. (9), $z_t^* \equiv -i\sum_k g_k z_k^* e^{i\nu_k t}$ is a stochastic noise satisfying $M\{z_t\} = M\{z_t z_s\} = 0$ and $M\{z_t z_s^*\} = \alpha(t, s)$ where $M\{\cdot\} \equiv \int \frac{d^2 z}{\pi} e^{-|z|^2} \{\cdot\}$ stands for the statistical mean over all the noise variable z .

Based on the NMQSD Eq. (9), the master equation of the double-mirror optomechanical system can be derived as (see Appendix A 2 for details)

$$\begin{aligned} \frac{\partial}{\partial t}\hat{\rho} &= -i[\hat{H}_{\text{S}}, \hat{\rho}] \\ &\quad + \sum_{i=1}^5 \sum_{j=1}^2 \left\{ \kappa_j F_i(t)(\hat{q}_j \hat{\rho} \hat{O}_i - \hat{\rho} \hat{O}_i \hat{q}_j) + \text{H.c.} \right\} \end{aligned} \quad (10)$$

where the operator \hat{O}_i are

$$\hat{O}_1 = \hat{q}_1, \hat{O}_2 = \hat{q}_2, \hat{O}_3 = \hat{p}_1, \hat{O}_4 = \hat{p}_2, \hat{O}_5 = \hat{a}^\dagger \hat{a}, \quad (11)$$

and the coefficients $F_i(t) = \int_0^t \alpha(t, s) f_i(t, s) ds$ ($i = 1, 2, 3, 4, 5$) are actually some TDCs (f_i are governed by a set of differential equations given in Appendix A 1). These TDCs $F_i(t)$ satisfy the following equations

$$\begin{aligned}
\frac{d}{dt}F_1 &= \frac{\gamma}{2}\kappa_1 - \gamma F_1 - i\Omega F_1 + 2\omega_1 F_3 - i\kappa_1 F_1 F_3 - i\kappa_2 F_1 F_4, \\
\frac{d}{dt}F_2 &= \frac{\gamma}{2}\kappa_2 - \gamma F_2 - i\Omega F_2 + 2\omega_2 F_4 - i\kappa_1 F_2 F_3 - i\kappa_2 F_2 F_4, \\
\frac{d}{dt}F_3 &= -\gamma F_3 - i\Omega F_3 - 2\omega_1 F_1 - i\kappa_1 F_3 F_3 - i\kappa_2 F_3 F_4, \\
\frac{d}{dt}F_4 &= -\gamma F_4 - i\Omega F_4 - 2\omega_2 F_2 - i\kappa_1 F_4 F_3 - i\kappa_2 F_4 F_4, \\
\frac{d}{dt}F_5 &= -\gamma F_5 - i\Omega F_5 + G_1 F_3 + G_2 F_4 - i\kappa_1 F_5 F_3 - i\kappa_2 F_5 F_4.
\end{aligned} \tag{12}$$

Given the master equation (10) with the TDCs determined by the Eqs. (12), one can evaluate the mean values of the physical observables such as the position and momentum. For an arbitrary operator \hat{A} , the mean value $\langle \hat{A} \rangle$ satisfies the relation

$$\frac{d}{dt}\langle \hat{A} \rangle = \frac{d}{dt}\text{tr}(\hat{A}\hat{\rho}) = \text{tr}(\hat{A}\frac{d}{dt}\hat{\rho}) \tag{13}$$

where the term $\frac{d}{dt}\hat{\rho}$ can be obtained from the master equation (10). Substituting Eq. (10) into Eq. (13), the dynamical equations governing the mean values of position and momentum of two movable mirrors can be derived. Since our focus is solely on the two mirrors, we

are only interested in four mean values $\langle \hat{p}_1 \rangle$, $\langle \hat{p}_2 \rangle$, $\langle \hat{q}_1 \rangle$, and $\langle \hat{q}_2 \rangle$. However, when computing these four mean values, $\langle \hat{a}^\dagger \hat{a} \rangle$ is involved in the calculation in order to obtain a set of closed equations. The details are presented in Appendix A 2. Therefore, we define a vector as $\vec{V} \equiv [\langle \hat{q}_1 \rangle, \langle \hat{q}_2 \rangle, \langle \hat{p}_1 \rangle, \langle \hat{p}_2 \rangle, \langle \hat{a}^\dagger \hat{a} \rangle]^T$, it satisfies a matrix equation

$$\frac{d}{dt}\vec{V} = \overleftrightarrow{M}\vec{V}, \tag{14}$$

where the coefficient matrix \overleftrightarrow{M} can be written as

$$\overleftrightarrow{M} = \begin{bmatrix} 0 & 0 & 2\omega_1 & 0 & 0 \\ 0 & 0 & 0 & 2\omega_2 & 0 \\ -2\omega_1 + \Im(\kappa_1 F_1) & \Im(\kappa_1 F_2) & \Im(\kappa_1 F_3) & \Im(\kappa_1 F_4) & -G_1 + \Im(\kappa_1 F_5) \\ -2\omega_2 + \Im(\kappa_2 F_1) & \Im(\kappa_2 F_2) & \Im(\kappa_2 F_3) & \Im(\kappa_2 F_4) & -G_2 + \Im(\kappa_2 F_5) \\ 0 & 0 & 0 & 0 & 0 \end{bmatrix}, \tag{15}$$

where $\Im(\cdot)$ indicates the imaginary part.

It is well known that chaos often occurs in a physical system whose dynamical equation contains nonlinear terms. The most famous example is the Lorentz equation [37]. Here, we derive a linear dynamical equation (14). According to the traditional theory, it is not likely to observe chaos in such a system. However, we also notice that the coefficients (TDCs) F_i ($i = 1$ to 5) satisfy a set of non-linear differential equations (12). This may provide the non-linearity for generating chaos in non-Markovian regime. Next, we will use analytical and numerical methods to show that the chaotic motions can be generated in this model purely by the non-Markovian back-reaction of the environment.

III. NON-MARKOVIAN ENVIRONMENT INDUCED CHAOS

Chaos describes the sensitivity to initial conditions in the dynamics. A quantitative measure of the exponen-

tial divergence of the dynamics is the Lyapunov exponent (LE) [36]. If two orbits are separated by the small distance ϵ_0 at the time $t = t_0$, then, at a later time t their separation is given by

$$\epsilon(t) \sim \epsilon_0 e^{\lambda t}, \tag{16}$$

where the λ is the LE [36, 70], quantifying the average growth of an infinitesimally small deviation of a regular orbit arising from a perturbation. In phase space, LE is a measure of the convergence and divergence rates of neighboring trajectories. A positive value of LE indicates chaotic dynamics and divergence from initial conditions. Conversely, a negative LE indicates trajectories in phase space converge to a common fixed point, suggesting regularity in system evolution. In a word, when LE exceeds zero, chaos occurs in the dynamics of the system.

Here we employ the Wolf's method of phase reconstruction [70] to calculate the maximum LE.

The wolf's method is simply divided into the following steps [73]:

(1) Taking an initial point in phase space as $Y(t_0)$, and let its nearest neighbor $Y_0(t_0)$, with the distance between the two points set as $A(t_0)$.

(2) Starting from time t_0 , we track the time evolution of these two points until the distance between them exceeds a specified value ε at time t_1 :

$$A'(t_1) = |Y(t_1) - Y_0(t_1)| > \varepsilon \quad (17)$$

(3) At this point, we keep $Y(t_1)$ and identify a new closest neighbor $Y_1(t_1)$ nearby, making sure the distance $|Y(t_1) - Y_1(t_1)| < \varepsilon$ and the angle between $A(t_1)$ and $A'(t_1)$ is minimized.

(4) The process is repeated until the end of the time series, accumulating a total of M iterations in the tracking evolution. The maximum Lyapunov exponent is then given by:

$$\lambda_1 = \frac{1}{t_M - t_0} \sum_{k=1}^M \ln \frac{A'_{t_k}}{A_{t_k-1}} \quad (18)$$

As we have discussed in Sec. II, the TDCs determine the dynamical behavior of the system, and the memory time $\tau = 1/\gamma$ plays a crucial role in the time evolution of the TDCs $F_i(t)$. To reveal the impact of τ on the chaos generation, we plot the maximum LE of physical observable $\langle \hat{q}_1 \rangle$ as a function of $\omega\tau$ and ωt in Fig. 2. The “red” regions with positive LE indicates a chaotic dynamics, while the “blue” regions with negative LE indicates no chaos. From our simulation, chaos generation strongly depends on the memory time $\tau = 1/\gamma$. Chaos only occurs when τ is large, i.e., the memory time is long. The early stage of evolution is not presented because it is common for a system to take some time to enter a chaotic dynamics.

Taking the fact that the dynamical equation (14) is in a linear format, the chaos generated with long memory time τ in Fig. 2 is somehow counter-intuitive. It is often believed that chaos is often accompanied by non-linearity. The only nonlinear factor in the equation is contained in the TDCs that satisfying Eqs. (12). Obviously, the TDCs provides the non-linearity for the chaos generation. Next, we will prove that the TDCs purely originate from the non-Markovian corrections. In Markovian limit, all the TDCs will be reduced to constants. As we have discussed in Eq. (7) and Eq. (8), small τ (large γ) corresponds to a Markovian environment. Mathematically, it is straightforward to check

$$\lim_{\gamma \rightarrow \infty} \alpha(t, s) \propto \delta(t, s), \quad (19)$$

leading to the TDCs become constants due to the properties of the δ -function (see Appendix A1)

$$F_i(t) \propto \int_0^t \delta(t, s) f_i(t, s) ds = \frac{f_i(t, t)}{2} = \text{constant}. \quad (20)$$

Therefore, the TDCs do not obey a set of nonlinear differential equations (12) any more.

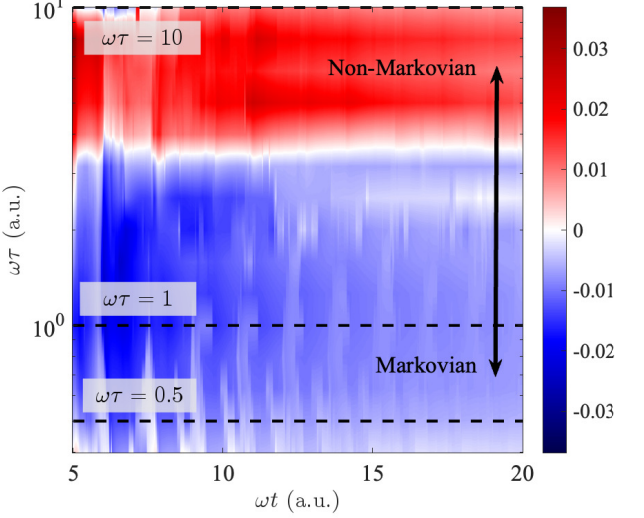


FIG. 2. The evolution of maximum LE for physical observable $\langle \hat{q}_1 \rangle$ with different correlation time τ . The initial conditions are $\langle \hat{q}_1 \rangle|_{t=0} = \langle \hat{q}_2 \rangle|_{t=0} = 1.1$ and $\langle \hat{p}_1 \rangle|_{t=0} = \langle \hat{p}_2 \rangle|_{t=0} = 0$ and $\langle \hat{a}^\dagger \hat{a} \rangle|_{t=0} = 2$. The parameters are $\omega_1 = \omega_2 = \omega = 1$, $\Omega = 0$, $G_1 = G_2 = 1$, and $\kappa_1 = \kappa_2 = 1$.

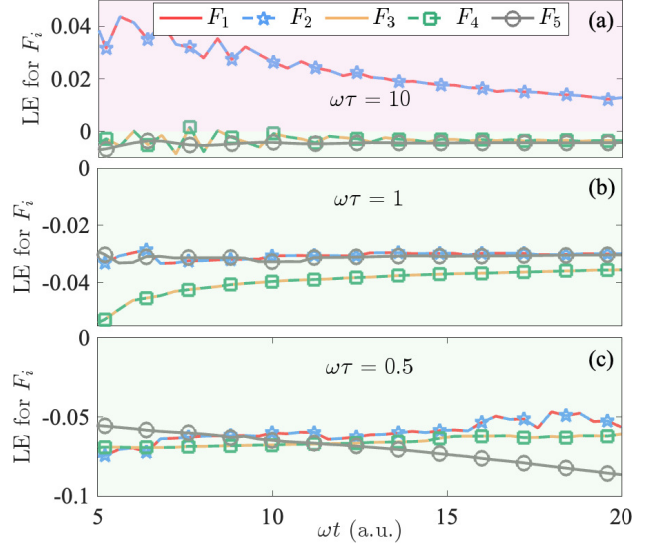


FIG. 3. Time evolution of maximum LE of the TDCs F_i with different correlation time τ . The parameters are the same as Fig. 2.

In summary, the TDCs provide the non-linearity for chaos generation in non-Markovian case, resulting in the positive LE region in Fig. 2. However, the TDCs are reduced into constants in Markovian limit, resulting in the disappear of non-linearity, further leading to the disappear of chaos in the negative LE region in Fig. 2.

To prove the theoretical analysis above, we numerically investigate the chaotic behaviors of the TDCs in Fig. 3. We select three particular values of $\omega\tau = 0.5$, $\omega\tau = 1$,

and $\omega\tau = 10$ which are marked by dashed lines in Fig. 2. For each given value of $\omega\tau$, The corresponding LE for F_i are plotted in Fig. 3. The chaotic behaviors of F_i are coincident with the chaotic behaviors of $\langle q_1 \rangle$. To be specific, in the case of long memory time indicated by $\omega\tau = 10$, chaos can be generated in subplot (a). As a comparison, in the cases of short memory time, presented in subplots (b) and (c), there are no chaos.

To further illustrate chaos and non-linearity is generated by the non-Markovian feedback effect other than the optomechanical couplings, we also numerically simulate the case of $G_1 = G_2 = 0$. In this scenario, the possibility that non-linearity is originated from the optomechanical couplings G_1 and G_2 is excluded, since the model is reduced to two harmonic oscillators coupled to a common environment [81, 82]. The figures and detailed discussion are presented in Fig. 6 in Appendix E, because the numerical plots are similar to Fig. 2 and Fig. 3. But we would like to emphasize that those results prove the chaotic dynamics we presented is not from optomechanical couplings. This is quite different from most existing studies on chaos in optomechanical systems [60, 83, 84].

From a physical perspective, the non-Markovian back-reaction of the environment provides non-linearity to the system. Mathematically, this non-linearity is reflected by the TDCs. Traditional research focusing on chaos generation in optomechanical system mainly concentrate on the radiation pressure associated with the parameter G , because this is a non-linear interaction. However, our results reveal an alternative provider of non-linearity, namely the non-Markovian feedback of the environment. We hope this opens a path to the study on chaos generation and we emphasize the important influence of environment should NOT be ignored.

Certainly, in some limiting cases, non-linearity is not a necessary condition for chaos. A famous example is the inverted harmonic oscillator (IHO) [85–87]. However, in most existing studies, chaos still arises from the properties of the IHO system itself. Our study shows the possibility of generating chaos from the interaction between a quantum system and its environment.

IV. INFLUENCE OF ENVIRONMENTAL PARAMETERS

In Sec. III, we investigate the chaos generation in double-mirror optomechanical system from a very special angle, i.e., chaos is purely induced by non-Markovian back-reaction of the environment. The importance of the environment in chaos generation has been demonstrated. In this section, we will further reveal the influence of the environmental parameters.

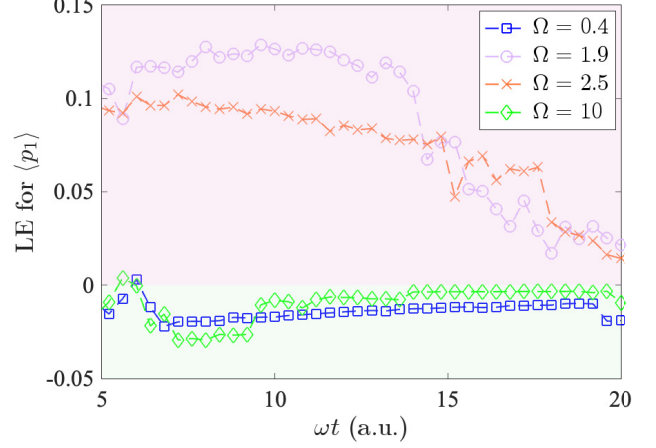


FIG. 4. Time evolution of LE of $\langle \hat{p}_1 \rangle$ with different central frequency Ω of the environment. The memory time τ is chosen as $\tau = 1$ ($\gamma = 1$), and the other parameters are the same as Fig. 2.

A. Central frequency

The properties of the environment are mainly characterized by two parameters in the correlation function $\alpha(t, s)$, the memory time τ and the central frequency Ω . The impact of τ has been extensively studied in Sec. III where we see the change of τ causes the transition from Markovian to non-Markovian regime. The chaos generation is a unique phenomenon that can be only observed in non-Markovian regime. Here, we show the influence of another parameter Ω . In Fig. 4, the LE of $\langle \hat{p}_1 \rangle$ is plotted for different values of Ω . It is observed that only for the case $\Omega \approx 2$, LE is positive, indicating chaos generation. For the other cases, LE is always negative in most regions of the time evolution.

According to Eq. (7), $|g(\nu)|^2 = J(\nu) \propto \frac{\gamma^2}{(\nu - \Omega)^2 + \gamma^2}$, only the bosonic modes with a frequency $\nu \approx \Omega$ have a strong interaction with the system, the other modes, especially those far from Ω , interact very weakly with the system. When the central frequency Ω is close to a particular frequency, a strong back-reaction is achieved between the system and environment. To understand the results in Fig. 4, one can recall the resonance phenomenon in classical physics as an analog. When the feedback has a particular frequency, it has the strongest impact on the system. Certainly, the numerical results in Fig. 4 reflect a very complicated multi-mode interactions satisfying a distribution in Eq. (7), the analog above is not rigorous.

If we consider a special case that the environment contains only a single mode (not the case in Fig. 4), it would be easier to capture the physical essence. Mathematically, in this limiting case, the Hamiltonian in Eq. (3) is reduced to $\hat{H}_B = \nu_1 \hat{b}_1^\dagger \hat{b}_1$ with $\nu_i = 0$ for all $i \neq 1$. Because there is only one mode, the central frequency is just $\Omega = \nu_1$. Besides, the interaction in Eq. (4) is also reduced to $\hat{H}_{\text{int}} = g_1(\kappa_1 \hat{q}_1 + \kappa_2 \hat{q}_2)(\hat{b}_1^\dagger + \hat{b}_1)$ with $g_i = 0$

for all $i \neq 1$. Now, the dynamics of the two mirrors is similar to the “vibration of coupled harmonic oscillator” which is widely discussed in the textbooks of classical mechanics [36]. When the frequency of the environment matches the frequency of the “normal mode” ω_{normal} of two mirrors, there is a strong energy exchange between the environment and the two mirrors. Otherwise, the energy exchange becomes smaller.

If the detuning between Ω and ω_{normal} is huge, the influence from the environment is very limited, as if the two mirrors are not interacting with the environment at all. Therefore, we only observe the chaos when $\Omega \approx 2$ in Fig. 4, because the two mirrors are approximately decoupled with the environment in huge detuning cases.

In summary, the central frequency of the environment is also crucial for the generation of chaos. When the central frequency is far detuned from the system frequencies, non-Markovian effect is weaken and chaos can not be generated.

B. Dissipation rate

The dissipation rate is another simple but important environmental parameter. In Fig. 5, We investigate the effects of asymmetric dissipation rates of two mirrors on the chaotic dynamics. In order to clearly show the optimal parameter range for chaotic phenomena, we plotted a contour map about the left mirror dissipation rate (κ_1) and the right mirror dissipation rate (κ_2). These plots offer a rich dynamics induced by the parameters κ_1 and κ_2 . According to Fig. 5, chaos generation only occurs when κ_1 and κ_2 are large. As we have analyzed in Sec. III, the nonlinearity for chaos generation is provided by the back-reaction of the environment, thus strong couplings κ_1 and κ_2 are necessary. It is straightforward to understand the absence of chaos in the region with small κ_1 and κ_2 by considering the limiting case that $\kappa_1 = \kappa_2 = 0$. In this case, the environment is decoupled. The matrix \hat{M} in Eq. (15) will be independent of TDCs $F_i(t)$, and the dynamical equation Eq. (14) is reduced to a linear equation. Consequently, the nonlinearity required for chaos disappear and no chaos generation observed.

The numerical results in Fig. 5 also reflect that the chaos generation is more sensitive to the parameter κ_1 . This is because we are plotting LE of $\langle \hat{p}_1 \rangle$. The dynamics of the left mirror is directly related to κ_1 , and the influence of κ_2 is indirectly. The LE of $\langle \hat{p}_2 \rangle$ is more sensitive to κ_2 according to our simulation (not presented).

In summary, we have discussed the influence of the environmental parameters, including the memory time τ , the central frequency Ω , and the dissipation rate κ_i . As we have mentioned in Sec. I, most existing studies focus on the nonlinear dynamical equations while our study focus on a linear dynamical equation. The nonlinearity is provided by the TDCs which are the consequence of non-Markovian corrections. Here, we would like to emphasize another difference between our research and most exist-

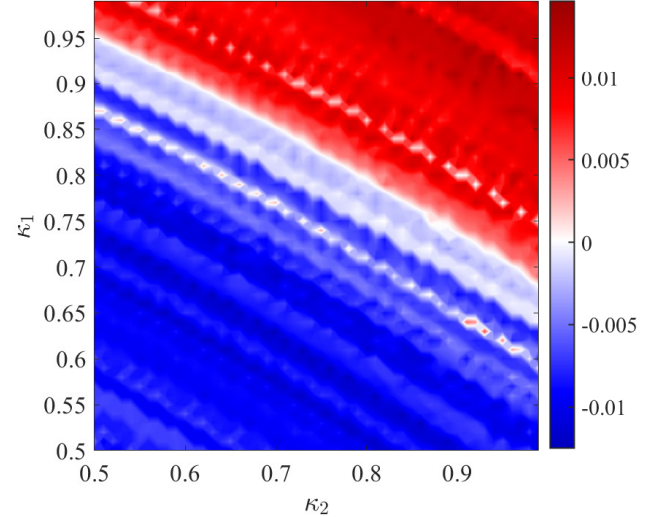


FIG. 5. The average of LE of $\langle \hat{p}_1 \rangle$ over $\omega t \in [5, 20]$. The parameters are $\gamma = 0.5$, $\Omega = 0$, $G_1 = G_2 = 1$, and $\omega_1 = \omega_2 = 1$. The initial conditions are $\langle \hat{q}_1 \rangle|_{t=0} = \langle \hat{q}_2 \rangle|_{t=0} = 1$, $\langle \hat{p}_1 \rangle|_{t=0} = \langle \hat{p}_2 \rangle|_{t=0} = 2$ and $\langle \hat{a}^\dagger \hat{a} \rangle|_{t=0} = 1$.

ing studies, i.e., we focus on the environmental parameters instead of system parameters. The results presented in this section show that the environmental parameters are equally important as the system parameters that are widely discussed in existing studies.

V. CONCLUSION

In this paper, we provide an insight into the effect of non-Markovian environment on chaotic dynamics in optomechanical systems. We derive the dynamical equation for the double-mirror optomechanical system. The non-linearity for chaotic dynamics is completely provided by the TDCs in the equation, which is the consequence of non-Markovian feedback effect. The full dynamics in Eq. (14) combined with Eq. (12) is, in fact, non-linear. The linear format of Eq. (14) is a formal mathematical result that serves to explicitly highlight the origin of nonlinearity: it is not embedded in the structure of the mean-value equation itself, but rather hidden in the TDCs, which are determined by the non-Markovian back-reaction of the environment. Thus, the chaos observed in this paper is purely generated by the non-Markovian effect. Both of our analytical and numerical results prove this conclusion and show that the chaos disappear in Markovian regime. Then, we further investigate the influence of the properties of the environment. We show that the environmental parameters including the memory time, the central frequency and the dissipation rate are crucial for the chaos generation.

The example presented in this paper open a new window for the investigation of chaotic behaviors. We have

demonstrated that the role of the environment in chaotic dynamics can be as significant as, or even more important than, the intrinsic properties of the system itself. Sometimes, the chaos can be purely generated by the non-Markovian effect of the environment. Future research may even focus on some linear system in the traditional theory, but coupled to a non-Markovian environment. The strong back-reaction from the environment may provide the non-linearity for the chaotic behaviors. We expect the results presented in this paper will stimulate greater interest in chaotic phenomena purely induced by non-Markovian environments.

ACKNOWLEDGMENTS

We thank the fruitful discussion with Dr. R. Luo. Y. Xia. was supported by the National Natural Science Foundation of China under Grant No. 62471143, the Key Program of National Natural Science Foundation of Fujian Province under Grant No. 2024J02008, and the project from Fuzhou University under Grant No. JG2020001-2. X. Zhao. was supported by Natural Science Foundation of Fujian Province under Grant No. 2022J01548.

Appendix A: Derivation of master equation

1. Equations for TDCs

In this subsection, we show the details of the derivation of the equations for the TDCs in Eq. (12) in the main text. First, we start from the derivation of the NMQSD equation. For the total state vector $|\psi_{\text{tot}}\rangle$ describing the quantum state involving both the system and the environment, it lives in the Hilbert space of H_{tot} and satisfies the Schrödinger equation

$$\frac{d}{dt}|\psi_{\text{tot}}\rangle = -i\hat{H}_{\text{tot}}|\psi_{\text{tot}}\rangle. \quad (\text{A1})$$

Using the Bargemann state basis $|z\rangle$ presented in the main text, one can take the time-derivative on both side of $|\psi_t(z^*)\rangle \equiv \langle z|\psi_{\text{tot}}(t)\rangle$. Noticing the relation $\hat{b}_i|z\rangle = z_i|z\rangle$ and $\hat{b}_i^\dagger|z\rangle = \frac{\partial}{\partial z_i}|z\rangle$, one can obtain Eq. (9) in the main text. To solve this equation, the functional derivative $\frac{\delta}{\delta z_s^*}$ can be replaced by a time-dependent operator as $\frac{\delta}{\delta z_s^*}|\psi_t(z^*)\rangle \equiv \hat{O}(t, s, z^*)|\psi_t(z^*)\rangle$ with the initial condition $\hat{O}(t = s, z^*) = (\kappa_1\hat{q}_1 + \kappa_2\hat{q}_2)$ [62]. Then, the NMQSD equation can be rewritten as

$$\begin{aligned} \frac{\partial}{\partial t}|\psi_t(z^*)\rangle &= [-i\hat{H}_{\text{S}} + (\kappa_1\hat{q}_1 + \kappa_2\hat{q}_2)z_t^* \\ &\quad - (\kappa_1\hat{q}_1 + \kappa_2\hat{q}_2)\bar{O}(t, z^*)]|\psi_t(z^*)\rangle, \end{aligned} \quad (\text{A2})$$

where $\bar{O}(t, z^*) = \int_0^t ds\alpha(t, s)\hat{O}(t, s, z^*)$. This is the fundamental equation governing the dynamics of the open

system without any approximation. The key to solve Eq. (A2) is finding the \hat{O} operator. There is a systematic approach to find the \hat{O} operator for arbitrary H_{S} in Refs. [22, 62, 88, 89]. Here, we only briefly review the procedure of solving \hat{O} operator.

According to the consistency condition $\frac{d}{dt}\frac{\delta}{\delta z_s^*}|\psi_t(z^*)\rangle = \frac{\delta}{\delta z_s^*}\frac{d}{dt}|\psi_t(z^*)\rangle$, the operator \hat{O} should satisfy the equation

$$\begin{aligned} \frac{\partial}{\partial t}\hat{O} &= [-i\hat{H}_{\text{S}} + (\kappa_1\hat{q}_1 + \kappa_2\hat{q}_2)z_t^* \\ &\quad - (\kappa_1\hat{q}_1 + \kappa_2\hat{q}_2)\bar{O}, \hat{O}] - \hat{L}^\dagger\frac{\delta}{\delta z_s^*}\bar{O}. \end{aligned} \quad (\text{A3})$$

Solving Eq.(A3), the exact \hat{O} operator for this particular model can be determined as

$$\hat{O}(t, s, z^*) = \sum_{i=1}^5 f_i(t, s)\hat{O}_i + \int_0^t ds' f_6(t, s, s')z_{s'}^*, \quad (\text{A4})$$

where the basis operators are

$$\hat{O}_1 = \hat{q}_1, \hat{O}_2 = \hat{q}_2, \hat{O}_3 = \hat{p}_1, \hat{O}_4 = \hat{p}_2, \hat{O}_5 = \hat{a}^\dagger\hat{a}, \quad (\text{A5})$$

and the coefficients satisfy the following equations

$$\begin{aligned} \frac{\partial}{\partial t}f_1 &= 2\omega_1f_3 - 2i\kappa_1F_1f_3 - i\kappa_1F_2f_4 + i\kappa_1F_3f_1 \\ &\quad + i\kappa_1F_4f_2 - i\kappa_2F_1f_4 - \kappa_1F_6, \end{aligned} \quad (\text{A6})$$

$$\begin{aligned} \frac{\partial}{\partial t}f_2 &= 2\omega_2f_4 - i\kappa_1F_2f_3 - i\kappa_2F_1f_3 - 2i\kappa_2F_1f_4 \\ &\quad + i\kappa_2F_3f_1 + i\kappa_2F_4f_2 - \kappa_2F_6, \end{aligned} \quad (\text{A7})$$

$$\frac{\partial}{\partial t}f_3 = -2\omega_1f_1 - i\kappa_1F_3f_3 - i\kappa_2F_3f_4, \quad (\text{A8})$$

$$\frac{\partial}{\partial t}f_4 = -2\omega_2f_2 - i\kappa_1F_4f_3 - i\kappa_2F_4f_4, \quad (\text{A9})$$

$$\frac{\partial}{\partial t}f_5 = G_1f_3 + G_2f_4 - i\kappa_1F_5f_3 - i\kappa_2F_5f_4, \quad (\text{A10})$$

$$\frac{\partial}{\partial t}f_6(t, s, s') = -i\kappa_1f_3(t, s)F_6(t, s') - i\kappa_2f_4(t, s)F_6(t, s'), \quad (\text{A11})$$

where $F_i(t) = \int_0^t \alpha(t, s)f_i(t, s)ds$ ($i = 1, 2, 3, 4, 5$), and $F_6(t, s') = \int_0^t \alpha(t, s)f_6(t, s, s')ds$. The boundary conditions for the coefficients are

$$f_1(t, t) = \kappa_1, \quad (\text{A12})$$

$$f_2(t, t) = \kappa_2, \quad (\text{A13})$$

$$f_3(t, t) = f_4(t, t) = f_5(t, t) = 0, \quad (\text{A14})$$

$$f_6(t, t, s') = 0, \quad f_6(t, s, t) = i\kappa_1 f_3(t, s) + i\kappa_2 f_4(t, s). \quad (\text{A15})$$

The differential equations for the coefficients $F_i(t)$ can be computed as

$$\begin{aligned} \frac{d}{dt} F_i(t) &= \frac{d}{dt} \int_0^t \alpha(t, s) f_i(t, s) ds \\ &= \frac{d}{dt} \int_0^t \frac{\Gamma\gamma}{2} e^{-(\gamma+i\Omega)|t-s|} f_i(t, s) ds \\ &= \frac{\Gamma\gamma}{2} f_i(t, t) + \int_0^t \frac{\Gamma\gamma}{2} \left[\frac{d}{dt} e^{-(\gamma+i\Omega)|t-s|} \right] f_i(t, s) ds \\ &\quad + \int_0^t \frac{\Gamma\gamma}{2} e^{-(\gamma+i\Omega)|t-s|} \frac{d}{dt} f_i(t, s) ds. \end{aligned} \quad (\text{A16})$$

Substituting Eq. (A6)-(A11) into Eq. (A16), the differential equations for the TDCs F_i in the main text can be derived as shown in Eq. (12).

It is worth to note that the dynamical equation is Eq. (A2) or the master equation (10). The equations (A6) to (A11) are just for the TDCs. In the main text we only consider the noise free \hat{O} operator $\hat{O}^{(0)} = \sum_{i=1}^5 f_i(t, s) \hat{O}_i$ as an approximate solution. This approximation is irrelevant to the Hilbert space of the system. Moreover, the accuracy of this approximation is validated in many existing examples [50, 88–91]. Particularly, in Ref. [92], the noise-dependent terms are proved to have an impact up to the fourth order (or higher) of g_i . When g_i is not extremely strong, it is always safe to drop the noise-dependent terms.

2. The non-Markovian master equation

In this subsection, we show the detailed derivation of the master equation (10) in the main text. The density operator ρ can be constructed by taking the statistical average over all the possible realization of the stochastic state vector $|\psi_t(z^*)\rangle$ as

$$\hat{\rho}_s = M\{|\psi_t(z^*)\rangle\langle\psi_t(z)|\} = \int \frac{d^2 z}{\pi} e^{-|z|^2} |\psi_t(z^*)\rangle\langle\psi_t(z)|. \quad (\text{A17})$$

Taking the time-derivative on both sides of Eq. (A17), one obtains

$$\begin{aligned} \frac{d}{dt} \hat{\rho} &= \frac{d}{dt} M\{|\psi_t(z^*)\rangle\langle\psi_t(z)|\} \\ &= M \left\{ \left[\frac{d}{dt} |\psi_t(z^*)\rangle \right] \langle\psi_t(z)| \right\} + M \left\{ |\psi_t(z^*)\rangle \frac{d}{dt} \langle\psi_t(z)| \right\} \\ &= M \left\{ \left[-i\hat{H}_S + \hat{Q}z_t^* - \hat{Q}\bar{O} \right] |\psi_t(z^*)\rangle\langle\psi_t(z)| \right\} \\ &\quad + M \left\{ |\psi_t(z^*)\rangle\langle\psi_t(z)| \left[iH_S + \hat{Q}z_t - \bar{O}^\dagger \hat{Q} \right] \right\}, \end{aligned} \quad (\text{A18})$$

where the notation $\hat{Q} = \kappa_1 \hat{q}_1 + \kappa_2 \hat{q}_2$ is used as a collective coupling operator for two mirrors. Since the operator

\hat{H}_S is independent of the noise z^* it is straightforward to obtain

$$\begin{aligned} M\{\hat{H}_S|\psi_t(z^*)\rangle\langle\psi_t(z)|\} \\ = \hat{H}_S M\{|\psi_t(z^*)\rangle\langle\psi_t(z)|\} = \hat{H}_S \hat{\rho}. \end{aligned} \quad (\text{A19})$$

If the operator \bar{O} is also noise independent (neglecting the \hat{O}_6 term), similar results can be obtained. Then, the only task is to compute the term $M\{z_t^*|\psi_t(z^*)\rangle\langle\psi_t(z)|\}$. Using the Novikov theorem [63, 64, 88], we have the following results

$$\begin{aligned} M\{|\psi_t(z^*)\rangle\langle\psi_t(z)|z_t\} &= M\{\bar{O}|\psi_t(z^*)\rangle\langle\psi_t(z)|\}, \\ M\{z_t^*|\psi_t(z^*)\rangle\langle\psi_t(z)|\} &= M\{|\psi_t(z^*)\rangle\langle\psi_t(z)|\bar{O}^\dagger\}. \end{aligned} \quad (\text{A20})$$

Finally, the master equation can be derived as shown in Eq. (10) in the main text.

In the derivation of the master equation, the z_t^* -noise dependent term associated with f_6 can be neglected. According to Ref. [92], the noise dependent term is typically several orders smaller than other terms. One can also follow the approach presented in Ref. [68] to derive the master equation with noise dependent term.

Appendix B: The differential equations for physical observables

In order to compute LE, one has to calculate the mean values of set of operators. Since $\frac{d}{dt} \langle \hat{A} \rangle = \text{tr}(\hat{A} \frac{d}{dt} \hat{\rho})$, one can obtain the following equations for the mean values

$$\frac{d}{dt} \langle \hat{q}_1 \rangle = 2\omega_1 \langle \hat{p}_1 \rangle, \quad (\text{B1})$$

$$\frac{d}{dt} \langle \hat{q}_2 \rangle = 2\omega_2 \langle \hat{p}_2 \rangle, \quad (\text{B2})$$

$$\begin{aligned} \frac{d}{dt} \langle \hat{p}_1 \rangle &= -2\omega_1 \langle \hat{q}_1 \rangle - G_1 \langle \hat{a}^\dagger \hat{a} \rangle \\ &\quad + i \sum_{i=1}^5 (-\kappa_1 F_i \langle \hat{O}_i \rangle + \kappa_1^* F_i^* \langle \hat{O}^\dagger \rangle), \end{aligned} \quad (\text{B3})$$

$$\begin{aligned} \frac{d}{dt} \langle \hat{p}_2 \rangle &= -2\omega_2 \langle \hat{q}_2 \rangle - G_2 \langle \hat{a}^\dagger \hat{a} \rangle \\ &\quad + i \sum_{i=1}^5 (-\kappa_2 F_i \langle \hat{O}_i \rangle + \kappa_2^* F_i^* \langle \hat{O}^\dagger \rangle), \end{aligned} \quad (\text{B4})$$

$$\frac{d}{dt} \langle \hat{a}^\dagger \hat{a} \rangle = 0. \quad (\text{B5})$$

To investigate the dynamics of the two mirrors the first four equations are enough. However, due to the optomechanical interaction, the photon number $\langle \hat{a}^\dagger \hat{a} \rangle$ is involved in Eq. (B3) and Eq. (B4). In order to solve $\langle \hat{p}_1 \rangle$ and $\langle \hat{p}_2 \rangle$, one has to also include $\langle \hat{a}^\dagger \hat{a} \rangle$ to form a set of closed equations which can be rewritten in a matrix form as shown in Eq. (14).

Appendix C: NMQSD equation in the presence of cavity leakage

In the main text, we assume the main decoherence channel is the damping of the two mirrors. Although the leakage of the cavity is relatively weak in most cases, it is still a possible source of decoherence. In this section, we present the procedure to derive the dynamical equations in the case that the cavity leakage is dominant.

When the cavity leakage is the primary system-environment interaction, the interaction Hamiltonian can be written as

$$\hat{H}_{\text{int}} = \sum_i g_i \hat{a} \hat{b}_i^\dagger + \text{H.c.} \quad (\text{C1})$$

Similarly, one can also introduce the same stochastic state vector $|\psi_t(z^*)\rangle = \langle z^*|\psi_{\text{tot}}(t)\rangle$ with stochastic variables z^* . Then, the NMQSD equation for this system can be derived as

$$\frac{\partial}{\partial t} |\psi_t(z^*)\rangle = \left[-i\hat{H}_S + \hat{a}z_t^* - \hat{a}^\dagger \int_{t_0}^t ds \alpha(t, s) \frac{\delta}{\delta z_s^*} \right] |\psi_t(z^*)\rangle, \quad (\text{C2})$$

with

$$z_t^* = -i \sum_i g_i z_m^* e^{i\omega_i t}, \quad (\text{C3})$$

The correlation function is

$$\alpha(t, s) = \sum_i |g_i|^2 e^{-i\omega_i(t-s)}. \quad (\text{C4})$$

To solve this equation, the functional derivative $\frac{\delta}{\delta z_s^*}$ can be replaced by a time-dependent operator as $\frac{\delta}{\delta z_s^*} |\psi_t(z^*)\rangle \equiv \hat{O}(t, s, z^*) |\psi_t(z^*)\rangle$ with the initial condition $\hat{O}(t = s, z^*) = \hat{a}$ [62]. Then, the NMQSD equation can be rewritten as

$$\frac{\partial}{\partial t} |\psi_t(z^*)\rangle = [-i\hat{H}_S + \hat{a}z_t^* - \hat{a}^\dagger \bar{O}(t, z^*)] |\psi_t(z^*)\rangle, \quad (\text{C5})$$

where $\bar{O}(t, z^*) = \int_0^t ds \alpha(t, s) O(t, s, z^*)$. According to the consistency condition $\frac{d}{dt} \frac{\delta}{\delta z_s^*} |\psi_t(z^*)\rangle = \frac{\delta}{\delta z_s^*} \frac{d}{dt} |\psi_t(z^*)\rangle$, the operator \hat{O} should satisfy the equation

$$\frac{\partial}{\partial t} \hat{O} = [-i\hat{H}_S + \hat{a}z_t^* - \hat{a}^\dagger \bar{O}, \hat{O}] - \hat{a}^\dagger \frac{\delta}{\delta z_s^*} \bar{O}. \quad (\text{C6})$$

Solving Eq. (C6), the \hat{O} operator for this particular model can be determined as

$$\hat{O}(t, s, z^*) = \sum_{i=1}^5 x_i(t, s) \hat{O}_i, \quad (\text{C7})$$

where the basis operators are

$$\hat{O}_1 = \hat{a}, \hat{O}_2 = \hat{q}_1 \hat{a}, \hat{O}_3 = \hat{p}_1 \hat{a}, \hat{O}_4 = \hat{q}_2 \hat{a}, \hat{O}_5 = \hat{p}_2 \hat{a}, \quad (\text{C8})$$

Substituting Eq. (C7) into Eq. (C6), one can obtain set of equation for the coefficients $x_i(t, s)$ which is similar to the differential equations shown in Eq. (A6)-(A11). Then, one can obtain the TDCs by following the similar procedure shown in Appendix A 1.

Finally, the master equation can be derived as

$$\frac{d}{dt} \hat{\rho} = -i[\hat{H}_S, \hat{\rho}] + [\hat{a}, \hat{\rho} \bar{O}^\dagger] - [\hat{a}^\dagger, \bar{O} \hat{\rho}_t]. \quad (\text{C9})$$

Appendix D: NMQSD equation for finite temperature

The temperature is also an important factor in the dynamics of the open system. In the main text, we assume the system is initially coupled to a vacuum state of the environment, which implies the initial temperature is zero. This is because the central topic of this paper is the non-Markovian feedback effect. The modification on the feedback caused by finite temperature can be studied in a future research. Here, in this section, we briefly show the procedure of deriving the dynamical equations in the case of finite temperature.

The general routine of solving finite temperature case is already set up in [65]. The fundamental idea is to introduce another fictitious bath $H_C = -\sum_k \omega_k c_k^\dagger c_k$, separated from all the other systems and environments. Thus, the fictitious bath does not affect the evolution of the original Hamiltonian. Then, by introducing Bogoliubov transformations, the initial thermal state for real bath $\rho_B(0) = e^{-\beta H_B}/Z$ is transformed into an effective vacuum state in the new basis. Eventually, a finite temperature problem with one real bath is mapped into a zero-temperature problem with two effective baths. According to [65], the NMQSD equation for finite temperature case is

$$\frac{\partial}{\partial t} |\psi_t(z^*, w^*)\rangle = [-i\hat{H}_S + \hat{R}z_t^* + \hat{R}^\dagger w_t^*, -\hat{R}^\dagger \bar{O}_1 - \hat{R} \bar{O}_2] |\psi_t(z^*, w^*)\rangle \quad (\text{D1})$$

where $\hat{R} = (\kappa_1 \hat{q}_1 + \kappa_2 \hat{q}_2) = \hat{R}^\dagger$ for this particular model and $z_t^* = -i \sum_k \sqrt{\bar{n}_k + 1} g_k z_k^* e^{i\omega_k t}$, $w_t^* = -i \sum_k \sqrt{\bar{n}_k} g_k w_k^* e^{-i\omega_k t}$ are two noise variables for those two effective baths after transformation. The two operators \hat{O}_1 and \hat{O}_2 satisfy the relations

$$\frac{\partial}{\partial t} \hat{O}_1 = [-i\hat{H}_S + \hat{R}z_t^* + \hat{R}^\dagger w_t^* - \hat{R}^\dagger \bar{O}_1 - \hat{R} \bar{O}_2, \hat{O}_1] - \hat{R}^\dagger \frac{\delta}{\delta z_s^*} \bar{O}_1 - \hat{R} \frac{\delta}{\delta z_s^*} \bar{O}_2, \quad (\text{D2})$$

$$\frac{\partial}{\partial t} \hat{O}_2 = [-i\hat{H}_S + \hat{R}z_t^* + \hat{R}^\dagger w_t^* - \hat{R}^\dagger \bar{O}_1 - \hat{R} \bar{O}_2, \hat{O}_2] - \hat{R}^\dagger \frac{\delta}{\delta w_s^*} \bar{O}_1 - \hat{R} \frac{\delta}{\delta w_s^*} \bar{O}_2, \quad (\text{D3})$$

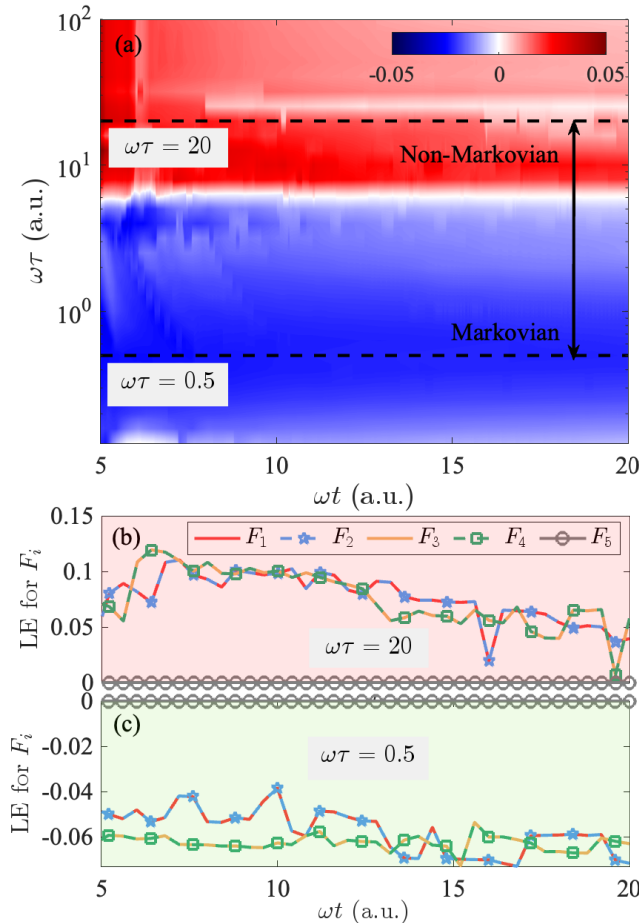


FIG. 6. (a) The evolution of maximum LE for physical observable $\langle \hat{p}_1 \rangle$ without optomechanical couplings ($G_1 = G_2 = 0$). (b) and (c) show the time evolution of maximum LE of the TDCs F_i with given memory time τ marked in (a), respectively. The initial conditions are $\langle \hat{q}_1 \rangle|_{t=0} = \langle \hat{q}_2 \rangle|_{t=0} = 0$ and $\langle \hat{p}_1 \rangle|_{t=0} = \langle \hat{p}_2 \rangle|_{t=0} = 1.1$ and $\langle \hat{a}^\dagger \hat{a} \rangle|_{t=0} = 2$. The parameters are $\omega_1 = \omega_2 = \omega = 1$, $\Omega = 0$, and $\kappa_1 = \kappa_2 = 2.02$.

with the initial conditions $\hat{O}_1(t, s = t, z^*, w^*) =$

\hat{R} and $\hat{O}_2(t, s = t, z^*, w^*) = \hat{R}^\dagger$, where $\hat{O}_i = \int_0^t \alpha_i(t, s) \hat{O}_i(t, s, z^*, w^*) ds$ ($i = 1, 2$). It is easy to note that in our particular model $\hat{R} = (\kappa_1 \hat{q}_1 + \kappa_2 \hat{q}_2) = \hat{R}^\dagger$, therefore two noises z_t^* and w_t^* as well as two \hat{O} operators \hat{O}_1 and \hat{O}_2 can be combined as a single noise and a single \hat{O} operator. Eventually, the NMQSD equation still keeps the form of Eq. (9), except the correlation function is slightly modified. For details, see [65].

Appendix E: Chaos generation without optomechanical couplings

Given the fact that the generation of chaos in optomechanical systems has been extensively studied [53, 58, 60], it is a well-established conclusion that optomechanical coupling can induce chaos. Consequently, upon obtaining the numerical results presented in Fig 2 and Fig 3, a natural question arises as to whether the chaotic phenomena depicted in these figures might be attributed to optomechanical couplings rather than being triggered by non-Markovian effects. Therefore, we present the numerical simulation for the case $G_1 = G_2 = 0$ in Fig. 6. The chaos generation without G_1 and G_2 excludes the possibility that chaos is originated from optomechanical couplings instead of non-Markovian feedback effects. Once more, the results in Fig. 6(b) and Fig. 6(c) confirm our analysis in Sec. III that non-Markovian corrections provide non-linearity in TDCs thus cause chaotic dynamics eventually.

Here, we have to emphasize that our results demonstrate for the possibility of chaos induced purely by non-Markovian effects with strong evidence. But the examples shown in the paper, including $G = 0$ and $G \neq 0$, are only special cases with chaotic dynamics. Certainly, non-Markovian environments with feedback effects cannot always ensure chaotic dynamics. The condition for chaos induced by non-Markovian environment is still an open question.

[1] R. Laje and D. V. Buonomano, *Nat. Neurosci* **16**, 925 (2013).

[2] F. Selmi, S. Coulibaly, Z. Loghmari, I. Sagnes, G. Beaudoin, M. G. Clerc, and S. Barbay, *Phys. Rev. Lett.* **116**, 013901 (2016).

[3] S. Coulibaly, M. G. Clerc, F. Selmi, and S. Barbay, *Phys. Rev. A* **95**, 023816 (2017).

[4] V. M. Eskov, O. E. Filatova, V. V. Eskov, and T. V. Gavrilenko, *Biophysics* **62**, 809 (2017).

[5] A. Argyris, D. Syrridis, L. Larger, V. Annovazzi-Lodi, P. Colet, I. Fischer, J. García-Ojalvo, C. Mirasso, L. Pesquera, and K. Shore, *Nature* **438**, 343 (2005).

[6] G. VanWiggeren and R. Roy, *Science* **279**, 1198 (1998).

[7] Y. Qiu, K. X. Yan, J. H. Lin, J. Song, Y. H. Chen, and Y. Xia, *New J. Phys.* **27**, 084503 (2025).

[8] I. Reidler, Y. Aviad, M. Rosenbluh, and I. Kanter, *Phys. Rev. Lett.* **103**, 024102 (2009).

[9] J. W. Yu, K. X. Yan, Y. Qiu, J. Song, Y. H. Chen, and Y. Xia, *Opt. Express* **33**, 26356 (2025).

[10] S. W. Xu, Z. Y. Zhang, J. T. Ye, Z. Z. Zhang, Y. Y. Guo, K. X. Yan, Y. H. Chen, and Y. Xia, *Opt. Express* **33**, 40755 (2025).

[11] K. Hirano, T. Yamazaki, S. Morikatsu, H. Okumura, H. Aida, A. Uchida, S. Yoshimori, K. Yoshimura, T. Harayama, and P. Davis, *Opt. Express* **18**, 5512 (2010).

[12] L. D'Alessio, Y. Kafri, A. Polkovnikov, and M. Rigol, *Adv. Phys.* **65**, 239 (2016).

[13] G. G. Gu, D. S. Li, Y. H. Chen, B. H. Huang, and Y. Xia, *Adv. Quantum Technol.* **8**, 2400518 (2025).

[14] G.-L. Zhu, C.-S. Hu, Y. Wu, and X.-Y. Lü, *Fundamental Research* **3**, 63 (2023).

[15] J. Wu, S.-W. Huang, Y. Huang, H. Zhou, J. Yang, J. Liu, M. Yu, G. Lo, D.-L. Kwong, S. Duan, and C. Wong, *Nat. Commun.* **8**, 15570 (2017).

[16] M. P. Fisher, V. Khemani, A. Nahum, and S. Vijay, *Annu. Rev. Condens. Matter Phys.* **14**, 335 (2023).

[17] Y. H. Chen, Y. Qiu, A. Miranowicz, N. Lambert, W. Qin, R. Stassi, Y. Xia, S. B. Zheng, and F. Nori, *Communications Physics* **7**, 5 (2024).

[18] G. Bouchez, T. Malica, D. Wolfersberger, and M. Sciamanna, *Phys. Rev. E* **103**, 042207 (2021).

[19] Z. Cao, Z. Xu, and A. del Campo, *Phys. Rev. Res.* **4**, 033093 (2022).

[20] L. Chen, W. Wu, F. Huang, Y. Chen, G.-S. Liu, Y. Luo, and Z. Chen, *Phys. Rev. A* **105**, L031501 (2022).

[21] J. Cornelius, Z. Xu, A. Saxena, A. Chenu, and A. del Campo, *Phys. Rev. Lett.* **128**, 190402 (2022).

[22] X. Zhao and Y. Xia, *Opt. Express* **33**, 619 (2025).

[23] N. Dowling, P. Kos, and K. Modi, *Phys. Rev. Lett.* **131**, 180403 (2023).

[24] J. Li and S. Chesi, *Phys. Rev. A* **109**, 053702 (2024).

[25] G. Madiot, F. Correia, S. Barbay, and R. Braive, *Phys. Rev. A* **104**, 023525 (2021).

[26] M. Martinez, O. Giraud, D. Ullmo, J. Billy, D. Guery-Odelin, B. Georgeot, and G. Lemarie, *Phys. Rev. Lett.* **126**, 174102 (2021).

[27] G. Park and S.-K. Kim, *Phys. Rev. B* **108**, 174441 (2023).

[28] E. Polyakov and N. Arefyeva, *Phys. Rev. A* **109**, 062204 (2024).

[29] S. Ray, A. Vardi, and D. Cohen, *Phys. Rev. Lett.* **128**, 130604 (2022).

[30] M. Tikhanovskaya, S. Sachdev, and A. A. Patel, *Phys. Rev. Lett.* **129**, 060601 (2022).

[31] A. B. Ustinov, A. V. Kondrashov, I. Tatsenko, A. A. Nikitin, and M. P. Kostylev, *Phys. Rev. B* **104**, L140410 (2021).

[32] R. Wanzenböck, S. Donsa, H. Hofstätter, O. Koch, P. Schlagheck, and I. Březinová, *Phys. Rev. A* **103**, 023336 (2021).

[33] M. Xu, F. Zhang, M. Pu, X. Li, X. Ma, Y. Guo, R. Zhang, M. Hong, and X. Luo, *Phys. Rev. Res.* **3**, 013215 (2021).

[34] Q. Zhai, R. L. Orbach, and D. L. Schlagel, *Phys. Rev. B* **105**, 014434 (2022).

[35] A. Uchida, K. Amano, M. Inoue, K. Hirano, S. Naito, H. Someya, I. Oowada, T. Kurashige, M. Shiki, S. Yoshimori, K. Yoshimura, and P. Davis, *Nat. Photonics* **2**, 728 (2008).

[36] H. Goldstein, C. Poole, and J. Safko, *Classical Mechanics (3rd Edition)*, 3rd ed. (Addison Wesley, San Francisco, 2001).

[37] E. N. Lorenz, *J. Atmos. Sci.* **20**, 130 (1963).

[38] S. Huang and G. S. Agarwal, *Phys. Rev. A* **83**, 043826 (2011).

[39] K. X. Yan, Y. Qiu, Y. Xiao, J. Song, Y. H. Chen, and Y. Xia, *Opt. Express* **33**, 39283 (2025).

[40] T. Rocheleau, T. Ndukum, C. Macklin, J. B. Hertzberg, A. A. Clerk, and K. C. Schwab, *Nature* **463**, 72 (2010).

[41] A. D. O'Connell, M. Hofheinz, M. Ansmann, R. C. Bialczak, M. Lenander, E. Lucero, M. Neeley, D. Sank, H. Wang, M. Weides, J. Wenner, J. M. Martinis, and A. N. Cleland, *Nature* **464**, 697 (2010).

[42] K. R. Brown, C. Ospelkaus, Y. Colombe, A. C. Wilson, D. Leibfried, and D. J. Wineland, *Nature* **471**, 196 (2011).

[43] J.-Q. Liao and C. K. Law, *Phys. Rev. A* **83**, 033820 (2011).

[44] F. Khalili, S. Danilishin, H. Miao, H. Müller-Ebhardt, H. Yang, and Y. Chen, *Phys. Rev. Lett.* **105**, 070403 (2010).

[45] H. Miao, C. Zhao, L. Ju, and D. G. Blair, *Phys. Rev. A* **79**, 063801 (2009).

[46] D.-G. Lai, X. Wang, W. Qin, B.-P. Hou, F. Nori, and J.-Q. Liao, *Phys. Rev. A* **102**, 023707 (2020).

[47] D.-G. Lai, W. Qin, B.-P. Hou, A. Miranowicz, and F. Nori, *Phys. Rev. A* **104**, 043521 (2021).

[48] R. Xu, D.-G. Lai, B.-P. Hou, A. Miranowicz, and F. Nori, *Phys. Rev. A* **106**, 033509 (2022).

[49] J. Huang, D.-G. Lai, C. Liu, J.-F. Huang, F. Nori, and J.-Q. Liao, *Phys. Rev. A* **106**, 013526 (2022).

[50] X. Zhao, *Opt. Express* **27**, 29082 (2019).

[51] D.-G. Lai, W. Qin, A. Miranowicz, and F. Nori, *Phys. Rev. Res.* **4**, 033102 (2022).

[52] X. Wang, W. Qin, A. Miranowicz, S. Savasta, and F. Nori, *Phys. Rev. A* **100**, 063827 (2019).

[53] K. Zhang, W. Chen, M. Bhattacharya, and P. Meystre, *Phys. Rev. A* **81**, 013802 (2010).

[54] D.-W. Zhang, L.-L. Zheng, M. Wang, Y. Zhou, and X.-Y. Lü, *Phys. Rev. A* **109**, 023529 (2024).

[55] J. Larson and M. Horsdal, *Phys. Rev. A* **84**, 021804(R) (2011).

[56] L. Bakemeier, A. Alvermann, and H. Fehske, *Phys. Rev. Lett.* **114**, 013601 (2015).

[57] D.-W. Zhang, C. You, and X.-Y. Lü, *Phys. Rev. A* **101**, 053851 (2020).

[58] X.-Y. Lü, H. Jing, J.-Y. Ma, and Y. Wu, *Phys. Rev. Lett.* **114**, 253601 (2015).

[59] G.-L. Zhu, X.-Y. Lü, L.-L. Zheng, Z.-M. Zhan, F. Nori, and Y. Wu, *Phys. Rev. A* **100**, 023825 (2019).

[60] Y. Ma, R. Zhao, X. Hou, J. Liu, M. Li, and X. Zhao, *Ann. Phys.* **535** (2023), 10.1002/andp.202200470.

[61] W. T. Strunz, L. Diósi, and N. Gisin, *Phys. Rev. Lett.* **82**, 1801 (1999).

[62] T. Yu, L. Diósi, N. Gisin, and W. T. Strunz, *Phys. Rev. A* **60**, 91 (1999).

[63] L. Diósi, N. Gisin, and W. T. Strunz, *Phys. Rev. A* **58**, 1699 (1998).

[64] W. T. Strunz and T. Yu, *Phys. Rev. A* **69**, 052115 (2004).

[65] T. Yu, *Phys. Rev. A* **69**, 062107 (2004).

[66] J. Jing and T. Yu, *Phys. Rev. Lett.* **105**, 240403 (2010).

[67] H. Yang, H. Miao, and Y. Chen, *Phys. Rev. A* **85**, 040101(R) (2012).

[68] Y. Chen, J. Q. You, and T. Yu, *Phys. Rev. A* **90**, 052104 (2014).

[69] G. Benettin, L. Galgani, A. Giorgilli, and J.-M. Strelcyn, *Meccanica* **15**, 9 (1980).

[70] A. Wolf, J. B. Swift, H. L. Swinney, and J. A. Vastano, *Physica D* **16**, 285 (1985).

[71] J. Ma, C. You, L.-G. Si, H. Xiong, J. Li, X. Yang, and Y. Wu, *Phys. Rev. A* **90**, 043839 (2014).

[72] L. Jin, J. Mei, and L. Li, *Appl. Phys. Lett.* **104** (2014), 10.1063/1.4870295.

[73] Y. H. Ma, X. W. Hou, R. Zhao, M. X. Li, and X. Y. Zhao, *Phys. Rev. E* **107**, 024220 (2023).

[74] C. K. Law, *Phys. Rev. A* **51**, 2537 (1995).

[75] H.-P. Breuer, E.-M. Laine, and J. Piilo, *Phys. Rev. Lett.* **103**, 210401 (2009).

[76] M. W. Y. Tu and W.-M. Zhang, *Phys. Rev. B* **78**, 235311

(2008).

[77] X. Zhao, Y.-H. Ma, and Y. Xia, *Phys. Rev. A* **105**, 042217 (2022).

[78] A. H. Safavi-Naeini, J. Chan, J. T. Hill, S. Gröblacher, H. Miao, Y. Chen, M. Aspelmeyer, and O. Painter, *New J. Phys.* **15**, 035007 (2013).

[79] V. Bargmann, P. Butera, L. Girardello, and J. R. Klauder, *Rep. Math. Phys.* **2**, 221 (1971).

[80] C. W. Gardiner and P. Zoller, *Quantum noise*, 3rd ed., Springer complexity (Springer, Berlin, 2010).

[81] J. P. Paz and A. J. Roncaglia, *Phys. Rev. Lett.* **100**, 220401 (2008).

[82] C.-H. Chou, T. Yu, and B. L. Hu, *Physical Review E* **77**, 011112 (2008).

[83] P. Chen, N. Yang, A. Couvertier, Q. Ding, R. Chatterjee, and T. Yu, *Entropy* **26**, 742 (2024).

[84] Y.-L. Xiang, X. Zhao, and Y. Xia, *Laser Phys.* **35**, 045204 (2025).

[85] L.-C. Qu, J. Chen, and Y.-X. Liu, *Phys. Rev. D* **105**, 126015 (2022).

[86] K. Hashimoto, K.-B. Huh, K.-Y. Kim, and R. Watanabe, *J. High Energy Phys.* **2020**, 068 (2020).

[87] L.-C. Qu, H.-Y. Jiang, and Y.-X. Liu, *J. High Energy Phys.* **2022**, 65 (2022).

[88] X. Zhao, W. Shi, L.-A. Wu, and T. Yu, *Phys. Rev. A* **86**, 032116 (2012).

[89] J. Jing, X. Zhao, J. Q. You, and T. Yu, *Phys. Rev. A* **85**, 042106 (2012).

[90] X. Zhao, J. Jing, B. Corn, and T. Yu, *Phys. Rev. A* **84**, 032101 (2011).

[91] Q. Mu, X. Zhao, and T. Yu, *Phys. Rev. A* **94**, 012334 (2016).

[92] J. Xu, X. Zhao, J. Jing, L.-A. Wu, and T. Yu, *J. Phys. A: Math. Theor.* **47**, 435301 (2014).